

THE IMPACT OF POSITIONAL INACCURACY ON 3D X-RAY IMAGE QUALITY *

L. Eley^{†,1}, C. P. Welsch¹, University of Liverpool, Liverpool, UK

A. Mavalankar, S. Wells, Adaptix Ltd, Oxford, UK

¹also at Cockcroft Institute, Warrington, UK

Abstract

X-ray imaging of both material and biological samples is a key application of synchrotrons and laser wakefield accelerators. However, it is possible that undiagnosed beam location offsets can impact the quality of the image created. This is particularly the case in 3D imaging, for which the 3D reconstructions require precise knowledge of the location at which each x-ray projection was taken. This study uses a low-energy x-ray imaging device designed to perform mobile digital tomosynthesis (DT), a modality of 3D x-ray imaging, for veterinary scanning to investigate the impact of this. An intentional offset is randomly applied of size 0.5 mm and 1 mm from the expected x-ray source position, and the quality of the reconstructed image is assessed for both the case where this offset is accounted for, and where it is not. From this, it is concluded that x-ray beams used for 3D imaging applications can have up to a 1 mm error without seeing large degradation in reconstructed image quality.

INTRODUCTION

The ability of synchrotrons and laser-wakefield accelerators to create x-ray beams to be used for imaging of both biological and material samples is an application of interest for this technology [1–5]. For biological samples, studies have found that the monochromaticity of such sources helps constrain patient dosage without the need of extra filtration layers [2], while for NDE studies, the ability to reach very high x-ray energies mean samples with high density can be quickly imaged. These findings apply to both 2D imaging, in which only a single image is taken, and 3D imaging, in which multiple projections of an x-ray source are required in order to for a 3D image to be mathematically reconstructed.

The most common mathematical approach to 3D image reconstruction is filtered backprojection [6, 7]. For each position of the source, a raytracing approach between the source and individual projection is used in order to average and transform the signal per pixel at different object heights. Therefore, with precise knowledge of where the source is for each image collected, a quasi-3D model can be mathematically created. This has the benefit over 2D images of being able to distinguish overlapping features more clearly.

Digital tomosynthesis (DT) is an example of a 3D imaging modality. Multiple projections of an X-ray source are used to create data that can be reconstructed using filtered backprojection, or similar techniques, into a 3D image. Adaptix

Ltd have developed a mobile DT device that uses a planar two-axis grid of x-ray emitters to create data that can be 3D reconstructed [8, 9].

The overlap of the reconstruction techniques for both this small DT device and that used for imaging from accelerators means that this study, performed on Adaptix Ltd's veterinary scanner [10] in Fig. 1, can be used to infer the importance of knowing the exact location of the x-ray beam output from accelerator x-ray sources.

METHOD

As stated, this study was performed using a veterinary scanner produced by Adaptix Ltd, as seen in Fig. 1 [9]. This device uses a transmission-type X-ray tube moved by mechanical stages to collect multiple projections at a voltage of 70 kV. The exact positions of the tube can be externally set, so for this investigation, a 6 x 6 grid of projections spaced by 10 mm was used. An image set was taken with no offset introduced. A second set was taken with a random positional offset of 0.5 mm introduced, and a third with a 1 mm offset randomly applied. To test the impact of these offsets in a way that could be quantified, 5 mm thick layer of PMMA with a grid of 25 equally spaced 1 mm aluminium spheres embedded within it from the Leeds Test objects TOMO IQ set [11] was imaged. Figure 1 displays both the veterinary scanner and the TOMO IQ phantom described above, which is placed on the detector.

To reduce error and improve image quality, all datasets taken had two frames per projection: one in which the phantom was present, and another where it was not. The image without the phantom present was subtracted from the one where it was to remove the effect of any features of the system from the images to be analysed. The images subtracted are known as 'air' frames, or for the sake of brevity, simply 'airs'.

The datasets containing offset projections were reconstructed four times. In the first, the images taken with the offset applied use the same air data and reconstruction positions, or 'keys', as if there were no offset. In the second, the offset keys are applied to the mathematical reconstruction, but the incorrect air data is subtracted. In the third, the correct air data is subtracted, but the uncorrected keys applied. Finally, both correct keys are used in the reconstruction and the correct air data for the position is applied. This approach was chosen under the assumption that a system where positional inaccuracies are present, it is likely both the airs and keys will be incorrect in the reconstruction, so the aim

* This work was jointly supported by Adaptix Ltd and the Science and Technology Facilities Council (STFC) under grant agreement ST/W006766/1.

† lauryn.eley@liverpool.ac.uk



Figure 1: The Adaptix veterinary scanner which has a source-to-image distance (SID) of 45 cm.

was to isolate these factors to see the contribution of each individually.

The standard image quality metrics [9]: signal-to-noise ratio (SNR), contrast-to-noise (CNR) and Z-resolution were then used to quantify the effect of having positional errors in the source position on the reconstructed image created. Figure 2 shows an example reconstruction plane (ie. a cross-section of the 3D reconstruction at a single height) with the aluminium spheres of the phantom chosen for this analysis indicated.

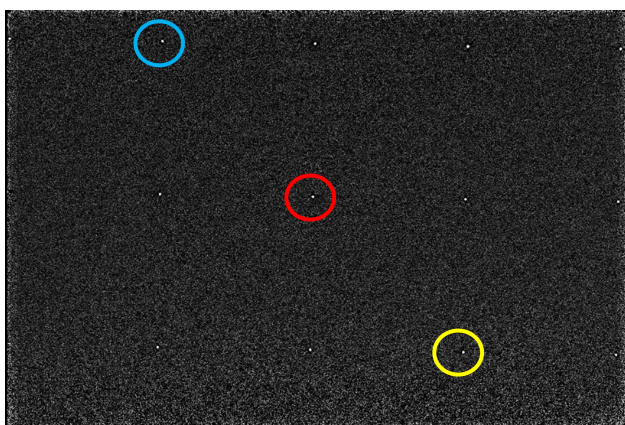


Figure 2: An example plane from the 3D reconstruction in which the three aluminium spheres used for analysis are highlighted.

RESULTS

CNR and SNR

Figure 3 shows the calculated SNR and CNR in-plane for the plane shown in Fig. 2. Both plots aim to demonstrate the calculated value of both ratios as a function of the offset applied to the images taken, with the legend indicating to what level this is accounted for in the subsequent reconstruction.

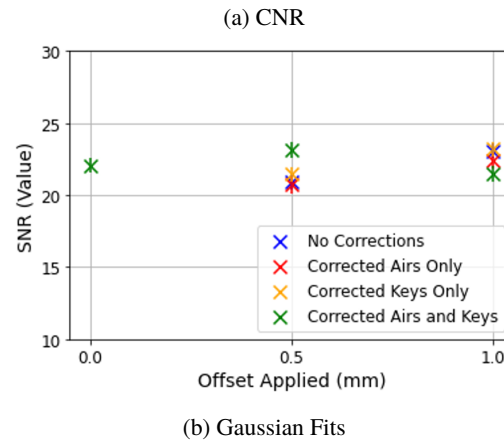
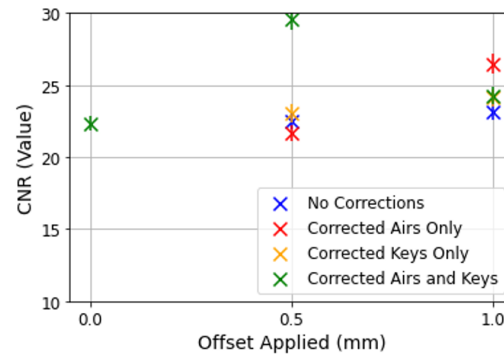


Figure 3: The CNR and SNR calculated for all iterations of the reconstructions as a function of applied offset.

For an offset of 0.5 mm, the SNR and CNR demonstrate an improvement when correct air data and positions ('keys') are applied in the reconstruction. Interestingly, it appears for both SNR and CNR that the combination that causes the worst quality reconstruction is that which uses the correct air data, but incorrect keys. This is, however, arguably within the error of both having no corrections and only correct keys applied, hence suggesting that all scenarios are equally as negatively impactful on the image quality.

For an offset of 1 mm, this is not the case. The scenario that shows the best image quality is that in which correct air data is applied, but correct keys are not. Having both corrections applied comes second to this, with the other two scenarios showing equally low image quality afterwards.

The final detail of note from this calculation is that the CNR appears to improve when an offset is applied when both the airs and keys are correct, compared to the 0 mm offset. This suggests irregular spacing of the x-ray source

may benefit imaging quality, though it must be noted, this does not appear to be the case in the SNR result.

Depth Resolution

Another important metric for determining 3D image quality is the depth resolution: that is, how quickly a feature stops being visible after the true height at which it is located. To calculate this, a line profile spanning the reconstruction height for the feature of interest is calculated, and the FWHM of the resultant Gaussian used to quantify this [9]. Figure 4(a) plots the values of FWHM calculated for each investigation from the gaussians shown in Fig. 4(b).

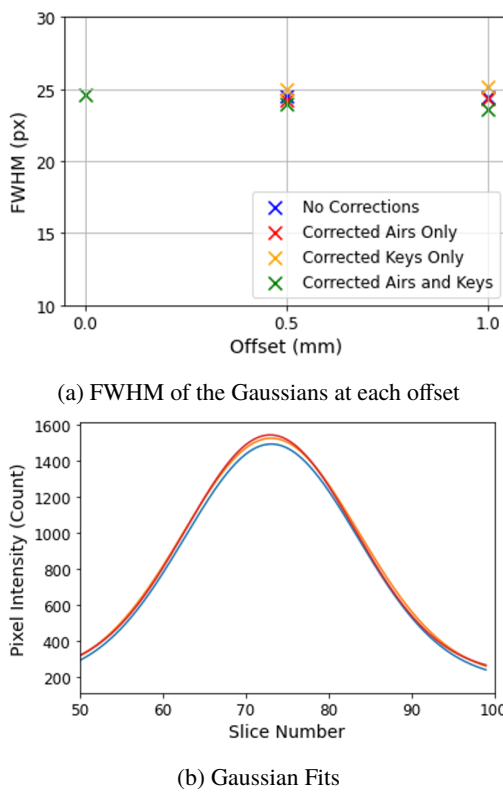


Figure 4: The depth resolution, expressed as the FWHM of the Gaussians plotted, calculated for all iterations of the reconstructions as a function of applied offset.

It can be seen from both figures that there is very little impact on applying the offset to the depth resolution of the reconstruction. This appears to be true for all iterations tested for this study, with the FWHM showing insignificant variation for all scenarios.

DISCUSSION

It is therefore seen that there appears to be no decisively significant impact of having inaccuracies in the position of an x-ray source within the magnitude of within 1 mm. Some trends are implied from the 0.5 mm CNR and SNR result that suggest an improvement of full accuracy in both position and air data, but there is not sufficient evidence to make this a certain conclusion of this work. Similarly, there is suggestion

that the CNR sees improvement from grid irregularity, but further work is required to show this. There is no impact on the depth resolution from positional inaccuracies, though this may have been expected, as the tomosynthesis angle has not changed between individual cases which is known to be the major factor influencing depth resolution for 3D image reconstructions in DT [12].

Further work using larger positional offsets in order to define at which point the inaccuracies do become significant would be useful to follow this study. Similarly, moving this work from a medical DT device to a synchrotron or laser wakefield facility would ensure the findings were directly applicable to the scenario being discussed, though as already stated, the overlap in imaging and reconstruction techniques make this a useful starting point.

CONCLUSION

There is no significant impact to 3D image quality metrics with positional inaccuracies of up to 1 mm. This suggests the acceptable range of error in knowledge of the location of an x-ray beam created by synchrotron facilities of at least 1 mm for imaging quality purposes. Further work is needed to quantify the maximum offset allowed before image quality is noticeably degraded.

REFERENCES

- [1] J. Albers, A. Svetlove, and E. Duke, "Synchrotron X-ray imaging of soft biological tissues—principles, applications and future prospects", *J. Cell Sci.*, vol. 137, no. 20, jcs261953, 2024. doi:10.1242/jcs.261953
- [2] J. Cole *et al.*, "Laser-wakefield accelerators as hard x-ray sources for 3D medical imaging of human bone", *Sci. Rep.*, vol. 5, no. 1, p. 13244, 2015. doi:10.1038/srep13244
- [3] C. A. Okolo, "A guide into the world of high-resolution 3D imaging: the case of soft X-ray tomography for the life sciences", *Biochem. Soc. Trans.*, vol. 50, no. 2, pp. 649–663, 2022. doi:10.1042/BST20210886
- [4] P. Tafforeau *et al.*, "Applications of X-ray synchrotron microtomography for non-destructive 3D studies of paleontological specimens", *Appl. Phys. A*, vol. 83, no. 2, pp. 195–202, 2006. doi:10.1007/s00339-006-3507-2
- [5] M. W. Westneat, J. J. Socha, and W.-K. Lee, "Advances in biological structure, function, and physiology using synchrotron x-ray imaging", *Annu. Rev. Physiol.*, vol. 70, no. 1, pp. 119–142, 2008. doi:10.1146/annurev.physiol.70.113006.100434
- [6] R. M. Joemai, W. J. Veldkamp, L. J. Kroft, I. Hernandez-Giron, and J. Geleijns, "Adaptive iterative dose reduction 3D versus filtered back projection in CT: evaluation of image quality", *Am. J. Roentgenol.*, vol. 201, no. 6, pp. 1291–1297, 2013. doi:10.2214/AJR.12.9780
- [7] Günter. Lauritsch and W. H. Härrer, "Theoretical framework for filtered back projection in tomosynthesis", in *Medical Imaging 1998: Image Processing*, vol. 3338, San Diego, CA, USA, Feb. 1998, pp. 1127–1137. doi:10.1117/12.310839

[8] M. Alabousi *et al.*, “Performance of digital breast tomosynthesis, synthetic mammography, and digital mammography in breast cancer screening: a systematic review and meta-analysis”, *J. Natl. Cancer Inst.*, vol. 113, no. 6, pp. 680–690, 2021. [doi:10.1093/jnci/djaa205](https://doi.org/10.1093/jnci/djaa205)

[9] S. Wells *et al.*, “Modelling the use of stationary, rectangular arrays of x-ray emitters for digital breast tomosynthesis”, in *Medical Imaging 2020: Physics of Medical Imaging*, vol. 11312, Houston, Texas, USA, Feb. 2020, pp. 179–191. [doi:10.1117/12.2548438](https://doi.org/10.1117/12.2548438)

[10] V. Y. Soloviev, K. L. Renforth, C. J. Dirckx, and S. G. Wells, “Meshless reconstruction technique for digital tomosynthesis”, *Phys. Med. Biol.*, vol. 65, no. 8, p. 085010, 2020. [doi:10.1088/1361-6560/ab7685](https://doi.org/10.1088/1361-6560/ab7685)

[11] A. Underwood, J. Law, and C. Clayton, “Reproducibility of leeds TOR (MAM) mammographic test object plates”, *Br. J. Radiol.*, vol. 70, no. 830, pp. 186–191, 1997. [doi:10.1259/bjr.70.830.9135446](https://doi.org/10.1259/bjr.70.830.9135446)

[12] T. Deller *et al.*, “Effect of acquisition parameters on image quality in digital tomosynthesis”, in *Medical Imaging 2007: Physics of Medical Imaging*, vol. 6510, San Diego, CA, USA, Feb. 2007, pp. 562–572. [doi:10.1117/12.713777](https://doi.org/10.1117/12.713777)